

**A NANOSIMS STUDY OF IRON-ISOTOPIC COMPOSITIONS IN PRESOLAR SILICON CARBIDE GRAINS.** K. K. Marhas<sup>1</sup>, P. Hoppe<sup>1</sup>, and A. Besmehn<sup>1,2</sup>, <sup>1</sup>Max-Planck-Institute for Chemistry, Cosmochemistry Department, D-55020 Mainz, Germany (kkmarhas/hoppe@mpch-mainz.mpg.de), <sup>2</sup>Research Centre Jülich, Central Department of Analytical Chemistry, D-52425 Jülich, Germany (a.besmehn@fz-juelich.de).

**Introduction:** Silicon carbide (SiC) is the best studied presolar mineral phase [1-3]. It is now well established that most of the presolar SiC (mainstream grains and the minor type Z and Y grains) originate from low-mass (1-3  $M_{\odot}$ ) asymptotic giant branch (AGB) stars. Also type II supernovae (SN) are believed to have contributed to the population of presolar SiC (X grains). Although low in abundance (about 1% of the SiC) the study of X grains has provided important insights into SN nucleosynthesis [e.g., 4, 5].

Only little isotopic information is available for the astrophysically diagnostic element Fe. To date Fe-isotopic compositions were measured for 4 mainstream grains, 9 unclassified grains, and 3 X grains by RIMS [6, 7]. These studies led to surprising results as  $^{54}\text{Fe}/^{56}\text{Fe}$  ratios in mainstream (and unclassified) grains are distinctly lower than solar, having an average  $\delta^{54}\text{Fe}$  of -130 ‰. Also  $^{57}\text{Fe}/^{56}\text{Fe}$  ratios are mostly lower than solar, although the depletions in  $^{57}\text{Fe}$  are less pronounced than those in  $^{54}\text{Fe}$ .  $^{58}\text{Fe}/^{56}\text{Fe}$  ratios, on the other hand, show a large scatter around the solar ratio. The lower than solar  $^{54}\text{Fe}/^{56}\text{Fe}$  has been interpreted to be the imprint of Galactic chemical evolution (GCE) [6]. While two of the X grains have  $^{54}\text{Fe}/^{56}\text{Fe}$  ratios in the range of mainstream grains, one X grain is enriched in  $^{54}\text{Fe}$  by about 200 ‰. Excesses of several 100 ‰ (with large analytical uncertainties) are seen for  $^{57}\text{Fe}$  and  $^{58}\text{Fe}$  in all X grains [6].

In order to get additional information on the Fe-isotopic composition of presolar SiC we have measured Fe-isotopic ratios in 8 grains with the NanoSIMS 50 ion microprobe at MPI for Chemistry, Mainz.

**Experimental:** SiC grains separated from the Sahara 97166 enstatite chondrite [8] were dispersed on gold foils. Prior to the NanoSIMS measurements the sample was screened by low-mass resolution ion imaging for  $^{30}\text{Si}/^{28}\text{Si}$  ratios with our Cameca IMS3f ion microprobe in order to locate the rare X grains. Four X grains identified by ion imaging were subsequently relocated in the NanoSIMS and measured together with 8 additional grains for C, N, and Si-isotopic compositions. Negative secondary ions of  $^{12}\text{C}$ ,  $^{13}\text{C}$ ,  $^{12}\text{C}^{14}\text{N}$ ,  $^{12}\text{C}^{15}\text{N}$ ,  $^{28}\text{Si}$ ,  $^{29}\text{Si}$ , and  $^{30}\text{Si}$  were measured in a combined multi-detection/peak-jumping mode using a defocussed (1-2  $\mu\text{m}$ )  $\text{Cs}^+$  primary ion beam of <1 pA.

Fe-isotopic ratios were measured in two of the X grains and in 6 grains of other types. Positive secondary ions of  $^{28}\text{Si}$ ,  $^{52}\text{Cr}$ ,  $^{54}\text{Fe}$ ,  $^{56}\text{Fe}$ , and  $^{57}\text{Fe}$  were ana-

lyzed in a combined multi-detection/peak-jumping mode with a defocussed ( $\sim 2 \mu\text{m}$ ) primary  $\text{O}^-$  beam of  $\sim 10 \text{ pA}$ .  $^{58}\text{Fe}$  was not included in the measurements because of its low isotopic abundance (0.31 ‰). High-resolution ion images, acquired with a focussed  $\text{O}^-$  primary ion beam ( $\sim 300 \text{ nm}$ ), were taken in order to check for possible contributions of Fe contamination to the grains's intrinsic Fe.

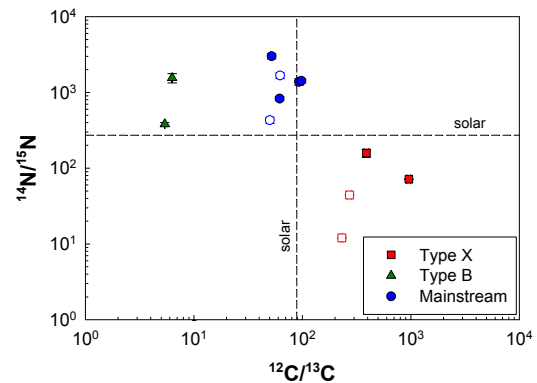


**Figure 1.** C- and N-isotopic compositions of presolar SiC grains from the Sahara 97166 enstatite chondrite. Errors are  $1\sigma$ . Filled symbols: Measured for Fe-isotopic composition; open symbols: not measured for Fe-isotopic composition.

**Results:** According to C-, N-, and Si-isotopic compositions, 2 of the SiC grains analyzed for Fe are of type B, 4 of the mainstream type, and 2 of type X (Table 1, Fig. 1). Fe/Si ratios are between  $4.7 \times 10^{-4}$  and 0.016 in the type B and mainstream grains, and around 0.01 in the X grains. In the mainstream grain SiC#13 there is a clear indication of Fe contamination as evidenced from a pronounced difference in the Si and Fe ion images (Fig. 2). Without this grain, Fe/Si ratios range up to 0.002 in B and mainstream grains, consistent with what was observed in previous studies [9]. The Fe/Si ratios in the X grains are higher by a factor  $>10$  than those previously studied [10]. However, at least for grain SiC#422-1 this seems to be an intrinsic feature because Fe is homogeneously distributed within the grain (Fig. 2).

The  $^{54}\text{Fe}/^{56}\text{Fe}$  and  $^{57}\text{Fe}/^{56}\text{Fe}$  ratios of the B and mainstream grains as well as of X grain SiC#294-3 are normal within  $2\sigma$  (Fig. 3). The mass-weighted average of  $\delta^{54}\text{Fe}$  in the B and mainstream grains (w/o SiC#13) is  $\delta^{54}\text{Fe} = -34 \pm 31 \text{ ‰}$  and  $\delta^{57}\text{Fe} = 9 \pm 24 \text{ ‰}$ . The only resolvable anomalies are seen for  $^{54}\text{Fe}/^{56}\text{Fe}$  and  $^{57}\text{Fe}/^{56}\text{Fe}$  in X grain SiC#422-1 (Fig. 3). But even here,

the anomalies are relatively small with excesses in  $^{54}\text{Fe}$  and  $^{57}\text{Fe}$  of only 30-40 %.

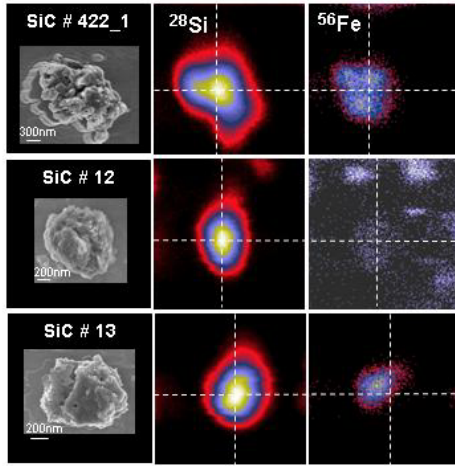


**Figure 2.** SEM and  $^{28}\text{Si}$  and  $^{56}\text{Fe}$  ion images of X grain SiC#422-1, and mainstream grains SiC#12 and SiC#13. Field of view is  $5 \times 5 \mu\text{m}^2$ .

**Discussion:** The  $^{54}\text{Fe}/^{56}\text{Fe}$  data of our B and mainstream grains fall at the upper end of the ratios measured by [6, 7] for mainstream grains. In AGB stars  $^{54}\text{Fe}$  and  $^{56}\text{Fe}$  are consumed by n-captures in the He intershell and the envelope abundances of these two isotopes change only marginally during the third dredge-up events. Contrary, large amounts of  $^{57}\text{Fe}$  are produced by n-capture in the He intershell and the third dredge-up will increase the envelope  $^{57}\text{Fe}/^{56}\text{Fe}$  ratio significantly [6]. The average  $\delta^{54}\text{Fe}$  and  $\delta^{57}\text{Fe}$  values of our B and mainstream grains are roughly compatible with model predictions ( $\delta^{54}\text{Fe} \sim 0$ ,  $\delta^{54}\text{Fe} = 50\text{-}150 \%$ ) for  $1.5\text{-}5 M_{\odot}$  AGB stars of solar metallicity and initially solar Fe-isotopic composition [6]. A better match, however, is achieved for  $\delta^{54}\text{Fe}_{\text{ini}} \sim -25 \%$  and  $\delta^{57}\text{Fe}_{\text{ini}} \sim -90 \%$ . In terms of GCE this would mean that  $^{54}\text{Fe}$  and  $^{57}\text{Fe}$  were depleted relative to solar isotopic abundances at the time the SiC grains formed.

In the different zones of type II SN Fe-isotopic compositions vary over many order of magnitudes. It was shown that the isotopic compositions of many elements in X grains can be satisfactorily explained if matter from the Si/S-, He/C, and He/N zones is mixed in variable proportions [4]. Small contributions from

the interior Ni zone, which probably provides the  $^{44}\text{Ti}$  seen in many X grains [4], will have a strong impact on the Fe-isotopic ratios because of very high concentrations of  $^{56}\text{Fe}$  and its radioactive progenitors. In view of the large variations expected for Fe-isotopic ratios in different SN zones, the close-to-normal ratios in the X grains of this study are surprising. Nevertheless, the Fe-isotopic signature of X grain SiC#422-1 is qualitatively consistent with that observed by [6] for one of their X grains and can be qualitatively understood in terms of the  $15 M_{\odot}$  type II SN model of [11] by mixing matter from the Si/S, He/C, and He/N zones, although the observed excess in  $^{54}\text{Fe}$  falls short of that expected for mixtures that can reproduce the Si-isotopic signature of SiC#422-1 (see Fig. 10 in [4]).

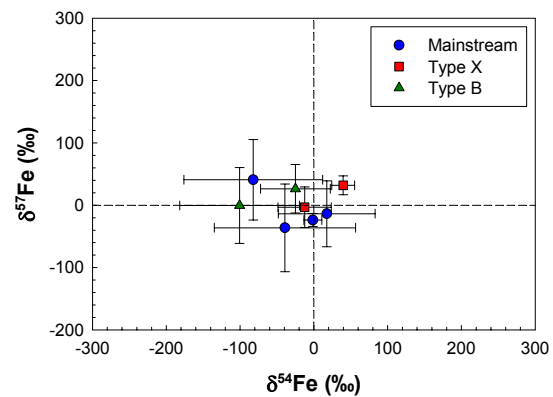


**Figure 3.** Fe-isotopic compositions of presolar SiC grains from the Sahara 97166 enstatite chondrite. Errors are  $1\sigma$ .

**Acknowledgements:** We thank J. Huth for his help with the SEM and E. Gröner for technical assistance.

**References:** [1] Zinner E. (1998) *Ann. Rev. Earth Planet. Sci.*, 26, 147. [2] Hoppe P. and Zinner E. (2000) *JGR*, 105, 10371. [3] Nittler L. R. (2003) *EPSL*, 209, 259. [4] Hoppe P. et al. (2000) *MAPS*, 35, 1157. [5] Pellin M. et al. (1999) *LPSC*, 30, abstr. #1969. [6] Davis A. M. et al. (2002) *LPSC*, 33, abstr. #2018. [7] Tripa C. E. et al. (2002) *LPSC*, 33, 1975. [8] Besmehn A. (2001) *PhD. thesis*, Universität Mainz. [9] Amari S. et al. (1995) *Meteoritics*, 30, 679. [10] Hoppe P. et al. (2001) *ApJ*, 551, 478. [11] Woosley S. E. and Weaver T. A. (1995) *ApJS*, 101, 181.

**Table 1.** C-, N-, Si-, and Fe-isotopic compositions and Fe/Si ratios in presolar SiC grains from Sahara 97166.

Grain	Type	$\delta^{29}\text{Si}$ (‰)	$\delta^{30}\text{Si}$ (‰)	$^{14}\text{N}/^{15}\text{N}$	$^{12}\text{C}/^{13}\text{C}$	$\delta^{54}\text{Fe}$ (‰)	$\delta^{57}\text{Fe}$ (‰)	Fe/Si $\times 10^{-3}$
SiC#12	Mainstream	$-3 \pm 4$	$3 \pm 5$	$3003 \pm 232$	$52.0 \pm 0.4$	$-82 \pm 94$	$41 \pm 65$	0.47
SiC#13	Mainstream	$-16 \pm 3$	$2 \pm 3$	$1380 \pm 137$	$93.1 \pm 0.6$	$-1 \pm 12$	$-24 \pm 10$	16.0
SiC#17	Mainstream	$-12 \pm 6$	$3 \pm 7$	$1423 \pm 87$	$98.1 \pm 1.3$	$18 \pm 66$	$-14 \pm 53$	4.7
SiC#408-7	Mainstream	$48 \pm 6$	$38 \pm 8$	$828 \pm 49$	$61.6 \pm 0.7$	$-39 \pm 96$	$-36 \pm 70$	1.24
SiC#10	B	$34 \pm 5$	$26 \pm 6$	$381 \pm 20$	$5.4 \pm 0.02$	$-101 \pm 81$	$-0 \pm 61$	1.91
SiC#14	B	$-8 \pm 5$	$24 \pm 6$	$1552 \pm 216$	$6.3 \pm 0.02$	$-25 \pm 47$	$26 \pm 39$	0.65
SiC#294-3	X	$-336 \pm 10$	$-491 \pm 11$	$158 \pm 19$	$389 \pm 19$	$-13 \pm 36$	$-3 \pm 33$	14.6
SiC#422-1	X	$-313 \pm 5$	$-498 \pm 5$	$71 \pm 1$	$959 \pm 36$	$40 \pm 16$	$32 \pm 15$	11.5